Available online at www.sciencedirect.com
SCIENCE DIRECT®
Remote Sensing of Environment 91 (2004) 27–46
Remote Sensing of Environment
www.elsevier.com/locate/rse

An evaluation of volcanic cloud detection techniques during recent significant eruptions in the western 'Ring of Fire'

Andrew Tupper[a,b,*], Simon Carn[c,1], Jason Davey[a,2], Yasuhiro Kamada[d,3], Rodney Potts[e,4], Fred Prata[f,5], Masami Tokuno[g,6]

[a] Bureau of Meteorology, Darwin, Northern Territory Region, Cascom Centre 0811, Casuarina, NT, Australia
[b] Monash University, Melbourne, VIC, Australia
[c] Joint Center for Earth Systems Technology, University of Maryland, Baltimore, MD, USA
[d] Tokyo Volcanic Ash Advisory Center, Japan Meteorological Agency, Haneda, Tokyo, Japan
[e] Bureau of Meteorology Research Centre, Melbourne, VIC, Australia
[f] CSIRO Atmospheric Research, Aspendale, VIC, Australia
[g] Hakodate Marine Meteorological Observatory, Japan Meteorological Agency, Hakodate, Japan

Received 25 July 2003; received in revised form 27 January 2004; accepted 18 February 2004

Abstract

We examined recent volcanic cloud events in the Western Pacific and Indonesian area, to validate the performance of remote sensing techniques used to support the International Airways Volcano Watch (IAVW). Five events were considered, during which eruptions from eight volcanoes injected ash into the upper troposphere or lower stratosphere. For one of the eruptions, at Miyakejima, Japan, at least five aircraft encountered volcanic ash clouds, and the cost to three operators alone exceeded US $12,000,000 in aircraft repairs, diversions, and lost operating time. We performed 'reverse' absorption and 'pattern analysis' using GMS-5/VISSR, MODIS and AVHRR data, and we examined TOMS SO_2 and Aerosol Index data, surface-based observations, pilot reports, and dispersion model output. Our results verify that the introduction of 'reverse' absorption using the geostationary GMS-5 platform significantly enhanced our capacity to monitor volcanic ash clouds in the region. In one case, we tracked an eruption cloud for approximately 80 h. The primary impediment to remote monitoring is the presence of overlying cloud, or substantial amounts of ice within the volcanic clouds. TOMS data showed success in identifying volcanic clouds during these conditions, but was limited by the infrequency of observations. More effective future operation of the IAVW relies on developing complementary methods of volcanic cloud remote sensing, and greatly increasing the amount and quality of available surface and air observations, including observations of precursor activity. An understanding of the likely future limitations of remote sensing techniques will aid in the refining of IAVW procedures.

Keywords: Satellite remote sensing; Volcanic ash detection; Volcanic eruptions; Aviation safety

1. Introduction

1.1. The International Airways Volcano Watch

Airborne volcanic ash causes significant damage and increased costs to the aviation industry annually. It has a demonstrated potential to cause major safety incidents, sometimes at great distances from the eruption responsible for the ash (eg Casadevall, 1994). In consequence, an international warning network has been progressively implemented, primarily over the last decade.

The International Airways Volcano Watch (IAVW) is a complex system that requires cooperation between world-

* Corresponding author. Bureau of Meteorology, Darwin, Northern Territory Region, Cascom Centre 0811, Casuarina, NT, Australia. Tel.: +61-8-8920-3867; fax: +61-8-8920-3829.
E-mail addresses: a.tupper@bom.gov.au (A. Tupper), scarn@umbc.edu (S. Carn), j.davey@bom.gov.au (J. Davey), ykamada@met.kishou.go.jp (Y. Kamada), r.potts@bom.gov.au (R. Potts), fred.prata@csiro.au (F. Prata), tokuno@met.kishou.go.jp (M. Tokuno).
[1] Fax: +1-410-455-5868.
[2] Fax: +61-8-8920-3829.
[3] Fax: +81-3-5756-0292.
[4] Fax: +61-3-9669-4660.
[5] Fax: +61-3-9239-4444.
[6] Fax: +81-138-46-1449.

0034-4257/$ - see front matter © 2004 Elsevier Inc. All rights reserved.
doi:10.1016/j.rse.2004.02.004

wide meteorological, aviation, and volcanological agencies, and exists under the International Civil Aviation Organisation (ICAO) and World Meteorological Organisation (WMO). Procedures and standards of service have evolved rapidly, to the point where a fledgling warning system is in place (ICAO, 2000, 2001).

As part of the IAVW, Volcanic Ash Advisory Centers (VAACs) have been established in nine locations, with areas of responsibility covering most of the world (ICAO, 2000). These centers provide guidance (Volcanic Ash Advisories) on the distribution and forecast movement of ash. Meteorological Watch Offices use this information when preparing warnings of significant meteorological conditions (SIGMETs) for aviation. Because of the extreme danger of volcanic ash and the need to maximize the speed and extent of communications, Volcanic Ash Advisories are also provided directly to airlines and are in the public domain (ICAO, 2000). The standards and procedures of the IAVW are set by ICAO and are negotiated between all IAVW participants, using informal and formal regional and international forums, and ultimately through the guidance of the IAVW Operations Group, which reports to the Air Navigation Commission (ICAO, 2003).

1.2. The IAVW in the western 'Ring of Fire'

Much of the world's volcanic activity is concentrated around the so-called 'Ring of Fire', which extends approximately around the perimeter of the Pacific Ocean. The western 'Ring of Fire', which includes Kamchatka (Russia), Japan, the Philippines, Indonesia, and Papua New Guinea, has had many of the world's major historical eruptions, and the majority of documented aircraft encounters with volcanic ash (ICAO, 2001). Many of these encounters are examined in Casadevall et al. (1996) and Johnson and Casadevall (1994). The VAACs responsible for monitoring this region are Tokyo (Japan), Darwin (Australia), Wellington (New Zealand), Washington, DC (USA), and Anchorage (USA).

These four countries have maintained robust consultative processes during the establishment of the IAVW in the region, involving volcanological agencies, airlines, aviation authorities, and meteorological services (eg Potts & Whitby, 1994). Recent discussion in the literature (Prata et al., 2001; Simpson et al., 2000, 2001, 2002) has, however, highlighted the need for improved communication between the 'operational' and 'research' communities regionally and worldwide.

1.3. Scientific and operational issues

A number of issues have been discussed in the recent literature. The complexities of volcanic cloud monitoring make it difficult to separate scientific from operational issues, or to treat all the possible issues fairly in one paper, but they include:

1.3.1. The concentration of ash required to measurably damage an aircraft

In promoting the IAVW, responsible aviation operators have developed the concept of 'complete avoidance' of volcanic ash (Campbell, 1994; Cantor, 1998; Rossier, 2002; Salinas, 1999). In reality, volcanic ash can be assumed to suffuse the entire atmosphere to some degree, and there is no definition of a 'safe' level of exposure (ICAO, 2000; FAA, 2001). There is evidence that some airlines are prepared to fly during situations where others will not; for example, in the cases of the Rinjani (Lombok, Indonesia) eruption of 1994 (Tupper & Kinoshita, 2003), and the 2002 Ruang (Sangihe Islands, Indonesia) eruption presented in this paper, Darwin VAAC meteorologists learned of specific cases where some airlines chose to fly through areas that contained detected ash cloud.

This issue has been a long-standing difficulty, but it came into prominence after the encounter of a NASA DC-8 research aircraft with a volcanic cloud from Hekla (Iceland) in 2000 (Grindle & Burcham, 2002, 2003; Pieri et al., 2002; Rose et al., 2003). The analysis of Grindle and Burcham (2003) suggested that the aircraft sustained damage from a volcanic cloud that could only be detected with sophisticated instruments; the implication being that aircraft flying in volcanically active areas, without such instruments, are probably sustaining undetected damage on many occasions. Space precludes a proper discussion of the Hekla analyses here, but the incident highlights current uncertainty about the damage caused by volcanic ash in low concentrations, and the importance of investigation of every reported encounter.

1.3.2. Detection of volcanic eruptions

Aircraft in the vicinity need to know about volcanic eruptions *immediately* that ash is at cruising levels, with a 5-min desired notification time often quoted (e.g. Ellrod et al., 2002; FAA, 2001; Simpson et al., 2002), based on the knowledge that an eruption cloud can reach cruising levels within five minutes of the eruption (FAA, 2001). ICAO (2000) set no actual lead-time standards; warnings are presumed to go out as soon as possible, which in practice has been known to take hours. Examination of individual events can suggest pragmatic ways to increase warning responsiveness and refine the IAVW.

1.3.3. The ability of remote sensing and other observational techniques to provide adequate data to verify the extent of dispersion of ash clouds

Techniques used for observing volcanic ash cloud dispersion are introduced in the next section; they have always been recognized as imperfect, and it is important to document as many cases as possible for the future development of the IAVW.

1.4. Purpose of this paper

The purpose of this paper is to evaluate the effectiveness of remote sensing of volcanic ash in the western Pacific

region, particularly during the extended GMS-5 ('Himawari') operations from 1995 to 2003. We present five cases that represent the more dangerous eruptions to have occurred in the region since 1995. We examine real-time satellite data used in meteorological operations, and also data normally available only for post-analysis. We describe a number of aircraft encounters with volcanic ash for these events, and we discuss the successes and failures of the IAVW for these events, focusing principally on remote sensing related issues.

2. Data and methods

2.1. Data

We used GMS-5 Visible Infrared Spin-Scan Radiometer (VISSR) data and US National Oceanic and Atmospheric Administration (NOAA) Advanced Very High Resolution Radiometer (AVHRR) data in High (1 km) Resolution Picture Transmission format from Bureau of Meteorology archives, AVHRR Local (1 km resolution) and Global (4 km) Area Coverage formats from the NOAA Satellite Active Archive (http://www.saa.noaa.gov/), and NASA Total Ozone Mapping Spectrometer (TOMS) and Moderate Resolution Imaging Spectroradiometer (MODIS) data. We sourced radiosonde observations from the Japan Meteorological Agency (JMA), the Australian Bureau of Meteorology (BOM), NOAA, and the UK Met Office, and used numerical and manual meteorological analyses from JMA and the BOM Darwin Regional Specialised Meteorological Centre. To aid our analyses we variously used dispersion model output from HYSPLIT (Draxler & Hess, 1998), the JMA 'Streamlined' Lagrangian volcanic ash dispersion model, and VAFTAD (Heffter & Stunder, 1993) output provided by the NOAA Air Resources Laboratory. We analyzed the infrared (IR) and visible satellite imagery using routines created in McIDAS 2002a (http://www.ssec.wisc.edu/software/mcidas.html) and ENVI 3.5 (http://www.rsinc.com/envi/).

2.2. Analysis of IR and visible imagery

For an overview of the use of remote sensing data in volcanology and volcanic cloud analysis, see Oppenheimer (1998) and Rose et al. (2000). Two principal methods of satellite analysis for volcanic clouds are used in operational work, 'pattern analysis' and 'reverse' absorption. Pattern analysis is the basis of operational satellite meteorology, where skilled analysts diagnose the nature of cloud features using single band IR and visible imagery in combination with other meteorological observations, numerical modeling and theoretical knowledge. Sawada (1987) produced a definitive analysis of past eruptions in the region using this technique, and the UK Met Office has been progressively implementing an automatic eruption detection system based on pattern analysis principles (Watkin et al., 2003).

The reverse absorption algorithm is described by Prata (1989a,b). The algorithm uses 11 and 12 μm brightness temperatures, to take advantage of the opposite absorption characteristics of water vapor or water/ice clouds and volcanic ash clouds at these wavelengths. Known limitations of the technique are summarized by Prata et al. (2001), Rose et al. (2000) and Simpson et al. (2000). For the cases presented here, the most relevant limitations are:

(i) The presence of substantial amounts of ice in ash cloud can partially or completely obscure the ash signal (Prata, 1989a; Rose et al., 1995).
(ii) Positive absorption from high amounts of water vapor (e.g. McMillin, 1975) can obscure the ash signal, an effect implicit in Prata (1989b), and shown for a Pinatubo eruption in Potts (1993). The effect can usually be detected using scatter diagram analysis (Prata et al., 2001), which Darwin VAAC performs in real-time operations.
(iii) Storms of mineral dust are generated over the Australian continent and very frequently over China, and can be observed using IR data (Ackerman, 1997; Iino et al., 2003; Kinoshita et al., 1999; Murayama et al., 2001; Sokolik, 2002, 2003). Although dust can be discriminated from volcanic aerosols during the day using multi-spectral techniques (Higurashi & Nakajima, 2002), there is some possibility of confusion between ash and dust using IR techniques only (Simpson et al., 2003). Archives of reverse absorption imagery of dust storms from China during 1997–present are kept by the Kagoshima Kosa Analysis Group, http://arist.edu.kagoshima-u.ac.jp/adust/kosa-e/kosa-e.htm (Iino et al., 2003); using these we have so far been unable to identify a major eruption and simultaneous dust storm for study.
(iv) False alarms from the technique can also occur in the presence of temperature inversions near the surface (Platt & Prata, 1993), in stratospheric thunderstorm cloud tops (Potts & Ebert, 1996), and in other circumstances summarized by Prata et al. (2001).

Pattern analysis and reverse absorption are complementary techniques, since pattern analysis, which requires sufficient gradient in the scene to distinguish volcanic from meteorological clouds (Sawada, 1987), works best for fresh, opaque eruption clouds clearly separated from other clouds, and reverse absorption requires the clouds to be semi-transparent and therefore usually in the dissipating stage. On this basis Prata et al. (2001) criticized the methodology employed by Simpson et al. (2000), who defined a reverse absorption failure rate based on cloud identified using pattern analysis. In practice, pattern analysis and reverse absorption are used together to produce operational analyses.

The differing channel separation, resolution, central wavelengths and channel widths of the different sensors also affect the reverse absorption results obtained for both ash and dust (Sokolik, 2002, 2003; Tokuno, 2000). Potts and Tokuno (1999) suggested that the GMS-5/VISSR sensor was useful for volcanic ash detection despite its poorer resolution (5 km at nadir) and channel separation compared to the NOAA/AVHRR sensor, because of the much higher temporal resolution of GMS-5 (half to one hourly). Merchant et al. (2003) compare well-calibrated ATSR-2 data to the less-well calibrated GMS-5 VISSR IR channels, while Koyama and Hillger (2003) show a low rate of degradation of the sensors during the period of interest. Tupper et al. (2003) compare MODIS, VISSR, and AVHRR retrievals over the 2002 Ruang eruption.

The Tokyo and Darwin VAACs use different implementations of the reverse absorption algorithm. Tokyo VAAC uses 12−11 μm images stretched for contrast, with many examples given in JMA (2003). Darwin VAAC uses 11−12 μm superimposed on an 11 μm image (for GMS/VISSR, labeled 'ΔT*/IR1' in this paper), to allow 'pattern analysis' on the same image. A simple despeckling filter reduces image noise, and the enhancement reduces 'false alarms' associated with high cloud tops (Potts & Ebert, 1996; Tupper et al., 2003) by imposing a more negative threshold for the reverse absorption algorithm to identify possible ash at very cold temperatures:

$$\text{for } T \geq 230 \text{ K}: \Delta T^* = \Delta T + c$$

$$\text{for } T < 230 \text{ K}: \Delta T^* = \Delta T + c + (230 - T(11\mu\text{m}))/f, \quad (1)$$

where T is the derived IR brightness temperature for the relevant channels, $\Delta T = T\,(11\ \mu\text{m}) - T\,(12\ \mu\text{m})$, and f and c are set empirically to correct for false alarms in cold thunderstorm tops and warm temperature/threshold problems, respectively. In preparing this paper, we considered each case using the Tokyo and Darwin algorithm variations, experimented with values of c and f, and then chose to present each case using the Darwin enhancement with $f = 12.5$ K (the operational default, empirically derived from Potts & Ebert, 1996) and $c = 0$ for all IR sensors. The difference between ΔT* and ΔT images was generally small except in the tropics, where the imagery was substantially improved through elimination of false alarms associated with very cold thunderstorm tops (Potts & Ebert, 1996; Tupper et al., 2003).

For each event, we prepared a temporal composite of all available VISSR ΔT*/IR1 images remapped to Mercator or Lambert Conformal projection, with the minimum ΔT* value during the period of the event shown at each point, and ΔT* values ≥ 0 excluded to aid clarity. This allows us to objectively determine the distance from the source for which each volcanic cloud gives a stronger reverse absorption signal than the maximum background 'noise'. There was some image-to-image variation in the overall ΔT*/IR1 magnitudes which we attribute to slight calibration or other quality control problems, and a few particularly 'noisy' and non-essential images were excluded from the composites; where the 'noise' has occurred during a critical phase of the eruption (for example, during the Miyakejima eruption), we retained all the data in the composite. We then annotated the composites with subjective analyses of the paths of all known volcanic clouds during the events.

2.3. Analysis of TOMS data

The TOMS instrument measures the albedo of the sunlit Earth at 6 ultraviolet (UV) wavelengths. Although designed to measure ozone (O_3) in the Earth's atmosphere, TOMS is also capable of mapping volcanic sulfur dioxide (SO_2) clouds due to similarities between the UV absorption spectra of O_3 and SO_2. The theoretical basis of the TOMS SO_2 retrieval algorithm is described by Krueger et al. (1995). TOMS UV radiance data are also used to produce an Aerosol Index (AI) that is sensitive to suspended matter, such as volcanic ash, smoke, dust and sulfate, in the atmosphere. The AI value is near zero in aerosol-free areas and for water clouds, and increases with aerosol optical depth and cloud altitude (Torres et al., 1998).

Since the inception of the TOMS program in 1978, four TOMS instruments have been flown on polar-orbiting satellites. For the recent eruptions under investigation here, the data were provided by ADEOS TOMS (operational Sept 1996–June 1997) and Earth Probe (EP) TOMS (operational July 1996–present). Typically, TOMS overpasses occur once daily at around local noon, but for the higher latitude Kamchatkan volcanoes (Shiveluch and Bezymianny; Table 1) more than one overpass occurred on each day owing to convergence of polar orbits. Where available, TOMS images for the studied eruptions can be found online at the TOMS volcanic emissions group website (http://skye.gsfc.nasa.gov).

Although TOMS data are usually available in near-real time through the World Wide Web, some of the events documented here were not fully analyzed at the time of each eruption but were re-analyzed for this paper. Along with SO_2 and AI data, TOMS O_3 data were also utilized, since they provide a means of distinguishing small amounts of SO_2 in otherwise indistinct volcanic clouds, owing to the similarities between SO_2 and O_3 referred to above. Volcanic SO_2 produces anomalous localized peaks in raw O_3 data, which can be identified as volcanic in origin when observed close to an erupting volcano since genuine O_3 rarely exhibits small-scale variations.

TOMS data has limited sensitivity in the lower troposphere; Sokolik (2002) questioned its value for monitoring mineral dust, which tend to be predominantly in the lowest few kilometers of the atmosphere. However, Simpson et al. (2003) used TOMS with a fair degree of success to track dust storms, and TOMS has been used successfully pre-

Table 1
Events selected for examination, in north–south order

Volcano(es)		Shiveluch	Bezymianny	Miyakejima	Ruang	Langila	Manam	Rabaul
Region		Kamchatka, Russia	Kamchatka, Russia	Izu Islands, Japan	Sangihe Islands, Indonesia	Papua New Guinea		
Dates		21–24 May 2001	6–8 Aug 2001	18–19 Aug 2000	25–26 Sep 2002	8–14 Feb 1997		
Meteorological summary		Deep, warm cored high pressure system centred over Kamchatka. Strong temperature inversions below 3 km.	Strong temperature inversions below 2 km. Significant polar/tropical interaction.	Warm and moist late-summer atmosphere. Eruption cloud travelled over developing sub-tropical low with widespread storm activity.	Moist tropical, scattered diurnal thunderstorms, but no organised maritime activity.	Active monsoon. Widespread thunderstorm activity with tops 15–17 km, following diurnal cycle of morning maritime and afternoon land convection. Poor meteorological data in area so wind fields poorly defined.		
Tropopause height (km)		12.5 ± 0.5	13 ± 0.5	17 ± 1	17 ± 1	17 ± 1		
Precipitable water (mm)		13 ± 5	20 ± 5	50 ± 5	52 ± 5	60 ± 10		
Satellite data used		VISSR, AVHRR, MODIS, EP TOMS	VISSR, AVHRR, MODIS, EP TOMS	VISSR, AVHRR#, MODIS#, EP TOMS	VISSR, AVHRR, MODIS, EP-TOMS	VISSR, AVHRR, ADEOS-TOMS, EP-TOMS		
Eruption characteristics & references		Smithsonian Institution (2001a); JMA (2003).	Smithsonian Institution (2001b). Explosive eruption, ash fall, lava flow.	Smithsonian Institution (2000, 2002a); Iino, Kinoshita, Koyamada et al., (2001); JMA (2003). Phreatomagmatic.	Smithsonian Institution (2002b); Tupper et al. (2003). First major eruption in Indonesia since Merapi, Nov. 1994.	Smithsonian Institution, 1997		
Maximum eruption height estimates (km above m.s.l.)	Ground	20	13	9	5*	10	7	7
	Pilot			12		8+		
	Brightness Temp.	>12@	>9	16@	16@	12	16@	15*
	Wind Drift Correl.	>12	12	15	>19			
	Other			16 (radar), 17.5 (lidar)	Shadow: 18.7 (VISSR), 21.5 (MODIS)	11 (encounter height)		
	Final	16 ± 4	12 ± 2	16.5 ± 1	20 ± 2	12 ± 2	16 ± 2	11 ± 4

The Langila, Manam, and Rabaul eruptions were simultaneous and are treated as a single event. Methods of eruption height estimates are described in the text. Notes: @ Minimum brightness temperature indicates eruption cloud near or above tropopause. # Some orbits unfavourable, data problems, or instrument failure. *Considered very approximate due to observational constraints.

viously for volcanic cloud studies (e.g. Constantine et al., 2000; Krotkov et al., 1999).

2.4. Case selection

The cases selected for analysis (Table 1) represent the more hazardous eruptions to have occurred recently in the region, across a wide range of meteorological conditions. Other volcanoes that were active during the period include Mayon (Philippines; JMA, 2003) and Ulawun (Papua New Guinea; Tupper & Kinoshita, 2003). Major lower level eruptions also occurred at Ruapehu (New Zealand; Potts & Tokuno, 1999) and Sakurajima (Japan), which has also had continuous minor activity (Iino, Kinoshita, Yano et al., 2001). Many volcanoes, such as Semeru (Java, Indonesia) or Suwanosejima (Japan), have been in a state of frequent low-level eruption, but the eruptions have often fallen below satellite resolution or have been completely obscured by cloud (Davey et al., 2003).

2.5. Height of eruptions

Eruption height is a critical parameter because it determines the eventual distribution of the ash. Table 1 summarizes estimates of eruption height from various sources. It is often difficult to reconcile eruption heights reported from the ground with satellite-observed heights (Sawada, 2002). Much of this can be attributed to the near-impossibility of making accurate height estimates of tall eruption clouds from observatories close to the volcano, as was possibly the case with the Ruang eruption considered here (Tupper & Kinoshita, 2003).

Volcanic cloud heights have been estimated by correlating IR brightness temperatures from opaque or near-opaque clouds with radiosonde soundings, by comparing cloud movement with atmospheric winds (Holasek et al., 1996; Oppenheimer, 1998), and examining pilot reports. For Ruang, we used shadow measurement (Prata & Grant, 2001) on Aqua/MODIS data. For the Ruang GMS-5/VISSR data, we also used an approximate shadow height method suitable for operational use, which avoids parallax complications (Oppenheimer, 1998) by comparing the cloud shadow with the shadows of nearby tropospheric meteorological clouds.

3. Results

3.1. Shiveluch, 21–24 May 2001

Fig. 1 summarizes the path of the Shiveluch eruption clouds, beginning at 0000 UTC on 21 May. Label A shows the path of the main ash cloud, produced from the 1309 UTC eruption on 21 May, and first visible on the 1337 UTC

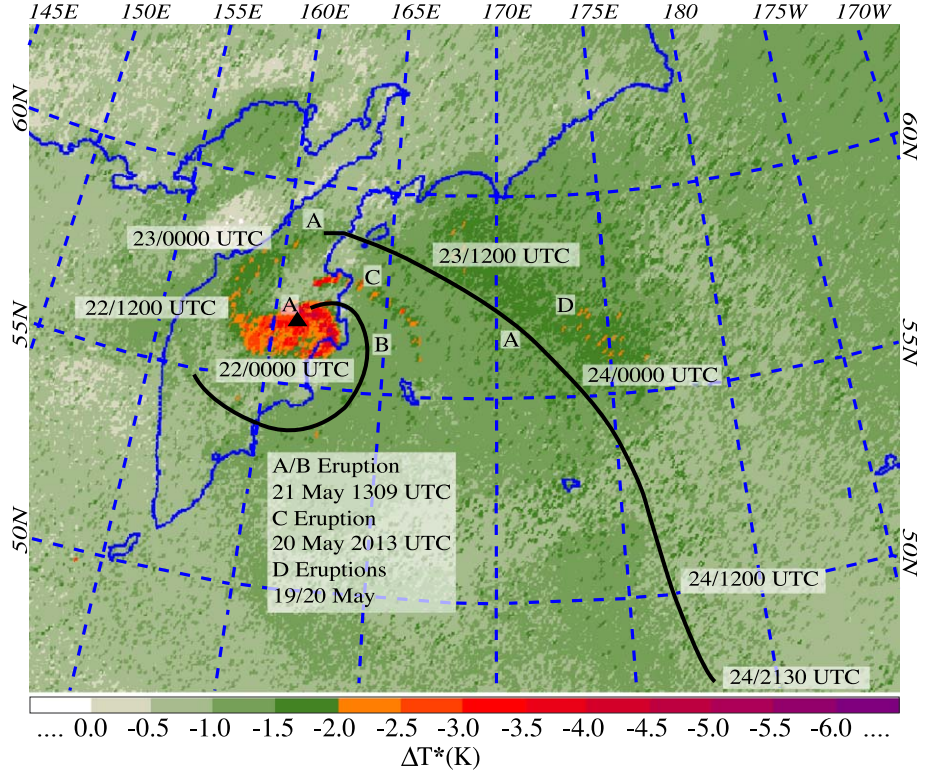

Fig. 1. Shiveluch eruption. Temporal composite of minimum hourly ΔT^*s from GMS-VISSR from 0037 UTC 21 May to 2137 UTC 24 May 2001, showing the approximate path A taken by the clouds from the eruption of 1309 UTC on 21 May, as well as other features B–D described in text. Minimum ΔT^*s during the period are shown at each pixel.

image (satellite times given are approximate overpass times). This ash cloud circled slowly over Kamchatka, before accelerating and moving to the southeast ahead of an intruding mid-latitude airmass, and became indistinct late on 24 May.

An area of minimum ΔT*s is located around D, close to the path of the dissipating cloud A. Analysis of earlier GMS animations (not shown) strongly suggests that this is residual ash from the earlier eruptions of 19 and 20 May, highlighting the complexity of ash clouds produced from eruptions with multiple explosive phases.

The main eruption cloud sheared with a portion (B) drifting to the southeast and then circling clockwise around the main body before becoming difficult to detect by 25 hours after the eruption. This cloud was more clearly visible on AVHRR and MODIS reverse absorption imagery than on VISSR. Ash from the 20 May 2013 UTC eruption also circled Kamchatka, at a slightly greater distance (C) and at an estimated height of 10–12 km.

There are some areas of 'false alarms' in the $-2\ \mathrm{K} < \Delta T^* < 0\ \mathrm{K}$ range. Visible imagery showed extensive areas of stratus, and temperature soundings confirm a low level inversion which, together with the relatively low precision of the data, was most likely responsible for the false alarms (Platt & Prata, 1993).

The exceptional visibility conditions for this event make a closer examination of the cloud signature worthwhile. Fig. 2 shows the coldest brightness temperature of the cloud over time, as well as the most negative ΔT within the cloud. The cloud was non-opaque from the first image, and the magnitude of ΔT increased over the next two hours as the cloud thinned further in parts. The decrease in brightness temperature as the cloud thinned in the first few hours after the eruption could reflect an increase in cloud height within the troposphere, but more likely indicates the thinning of a stratospheric cloud to show colder layers closer to the tropopause.

From about 00 UTC on 22 May, 12 hours after the eruption, the cloud became impossible to track using single channel IR imagery, and its position was taken to be that of the strongest reverse absorption signal. The IR temperature shown after that point varies with the temperature of the underlying surface, as is evident from the 'spike' on 23 May as the cloud transited warm land during the day.

From Figs. 1 and 2, the time for which the reverse absorption imagery unambiguously tracked the main body of the ash cloud (with values clearly higher than background noise) was about 36 h. Careful post-analysis of individual images shows the track continuing for approximately another 44 h. For this eruption, with a dry atmosphere and no noteworthy water/ice clouds, a skilled analyst can potentially track the ash cloud for 12 h using 'pattern analysis', and about 80 h in total using the split window method with GMS-5 data only.

Fig. 3 compares ΔTs for VISSR and AVHRR data at 1537 UTC and 1547 UTC respectively on 21 May, and shows the relevant IR and IR/ΔT* images. At this stage, the cloud was thinning and shearing, with the central portion still relatively opaque and giving near-zero ΔTs (the ΔT* formulation used increases the ΔTs in the IR/ΔT* image centers by about 1 K). The GMS-5 data are distorted due to parallax effects that are exaggerated with the height of the cloud, but overall the two sensors compare extremely well. The number of GMS points clustered just below the zero line on the scatter diagram reflects the lower resolution of the data, especially at high latitudes.

EP TOMS detected no SO_2 from this event. An AI image from 2314 UTC on 21 May showed aerosols associated with cloud A, a weak signal corresponding to

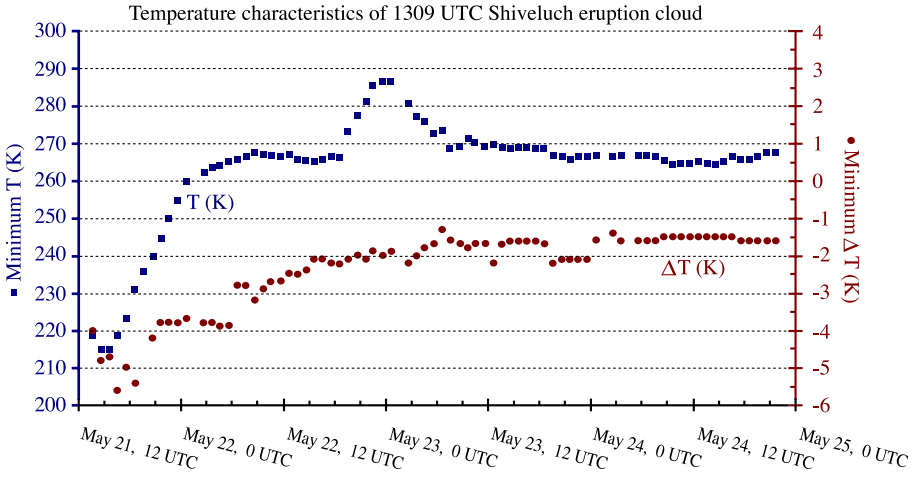

Fig. 2. Minimum brightness temperature from IR imagery and minimum ΔT from reverse absorption imagery of the Shiveluch eruption cloud from 1309 UTC 21 May 2001, showing the decay of the cloud signature over time. After 00 UTC on 22 May the brightness temperature of the cloud could not be independently tracked on IR images, so the temperature given is from the location of the most negative ΔT* on reverse absorption images.

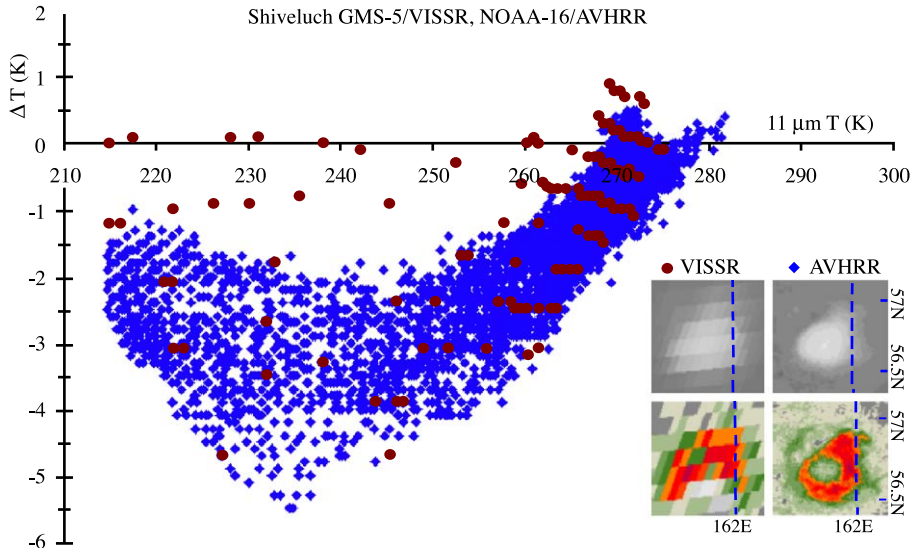

Fig. 3. Scatter diagram of Δ*T*s over Shiveluch cloud for NOAA-16/AVHRR and GMS-5/VISSR. Images shown are (top row) GMS-5/VISSR, IR1, 1537 UTC (left), and NOAA-16/AVHRR T4, 1547 UTC (right). Bottom row; corresponding Δ*T**/IR images. The data used in the scatter diagrams is from the same area as the images. Scaling for negative Δ*T**s is as for Fig. 1.

cloud C, and aerosols over northern Kamchatka which were not apparent on other imagery but which may be associated with earlier eruptions. A 0007 UTC pass from 22 May gives a similar result, confirming the presence of an ash cloud south of the volcano, and with aerosols again over northern Kamchatka. No TOMS images clearly detected ash after 22 May.

3.2. Bezymianny, 6–8 August 2001

The path of the ash transported from the Bezymianny eruption is summarized in Fig. 4. False alarms were, as for the Shiveluch eruption, associated with low level stratocumulus or clear air, but the ash cloud could be tracked unambiguously for about 30 h.

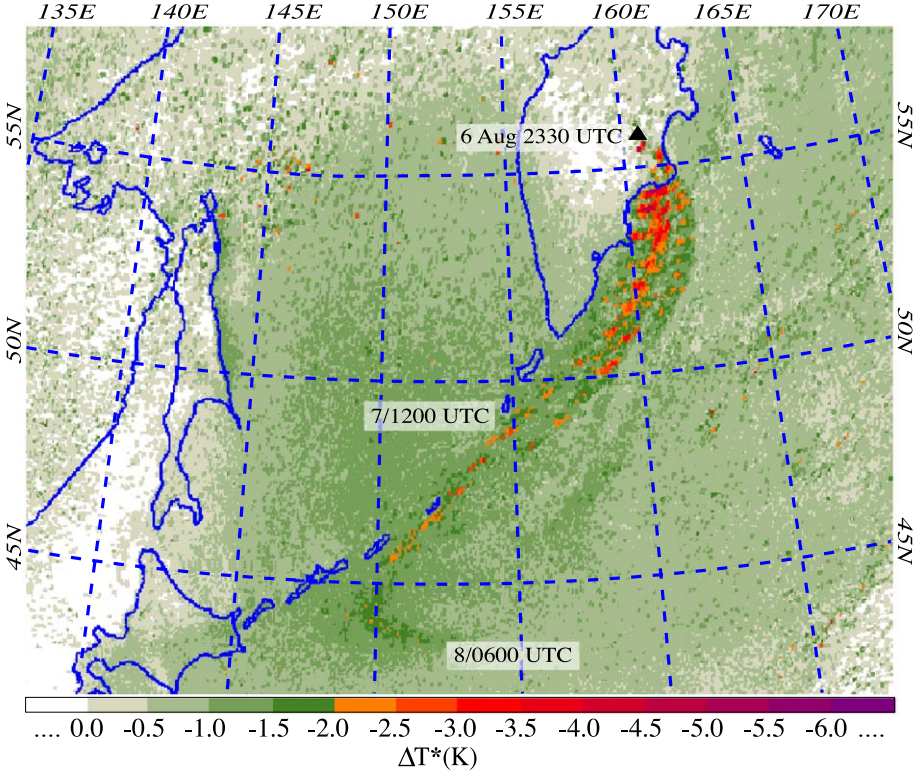

Fig. 4. GMS temporal composite for 2228 UTC 6 August 2001 Bezymianny eruption, from 2235 UTC 6 August to 0637 UTC 8 August.

The eruption started at 2328 UTC on 6 August (Smithsonian Institution, 2001b). At 2338 UTC a GMS/VISSR image showed a small cloud with possible ash detected by the split-window image in the center. At 2345 UTC the eruption was observed to a height of 13 km above MSL. EP TOMS flew over the Bezymianny region at 2358 UTC on 6 August and AI data showed an aerosol signal at the location. The next TOMS overpass did not occur until 2312 UTC on 7 August, and showed no aerosol signal. Hence, TOMS missed the main period of cloud transport southwest towards the Kuriles although it was the first satellite sensor to clearly show the ash cloud. Again, no SO_2 was detected by TOMS for the event; in this case the unfavorable orbits and the mainly tropospheric altitude of the cloud may have affected detection.

This case is notable because of the deformation of the cloud as it moved south during a period of polar/tropical airmass interaction, with lower level cloud moving more slowly and taking a more easterly track, and possibly some stretching deformation occurring as the flow accelerated. At maximum extent the cloud mass stretched 1700 km SSW of the eruption and almost to Hokkaido, effectively closing that airspace. An eastward 'turn' is evident at the southern extent of the ash cloud as the ash encountered the upper outflow from Typhoon 'Man-Yi', which was steadily moving northward and beginning to dissipate. After that point, observation of the now diffuse ash cloud was curtailed by it mixing with, or being obscured by, the cirrus shield associated with the storm outflow. Some ash would certainly have been carried eastwards across the Pacific.

3.3. Miyakejima, 18–19 August 2000

The Miyakejima eruption was a considerably more complicated event than the preceding examples. Ground based observations of the event (radar, video, eye witness reports) are widely available, but satellite observation was limited by a relative lack of AVHRR passes over the eruption cloud, and by Terra/MODIS instrument failure during the 18th. Fig. 5 is a temporal composite of GMS split-window data, with the approximate positions of the known aircraft encounters and the paths of the ash clouds indicated. Hourly VISSR reverse absorption images are shown by Iino, Kinoshita, Koyamada et al. (2001), JMA (2003) and Kinoshita et al. (2003).

At least five aircraft are known to have encountered the ash clouds (Table 2), with at least two sustaining life-threatening damage (loss of electronic engine controls, loss of forward visibility), and total costs probably well over US$12 million.

Four ash cloud tracks have been indicated on Fig. 5. Path A shows a strong, discrete ash signal that moved south–southwest at approximately 9 m/s and an altitude of above 15 km, becoming lost over the cloud of a developing low pressure system (which followed the path J) at 1840 UTC. The EP TOMS pass at 0221 UTC on 19 August showed a strong SO_2 signal near the area where this ash would be

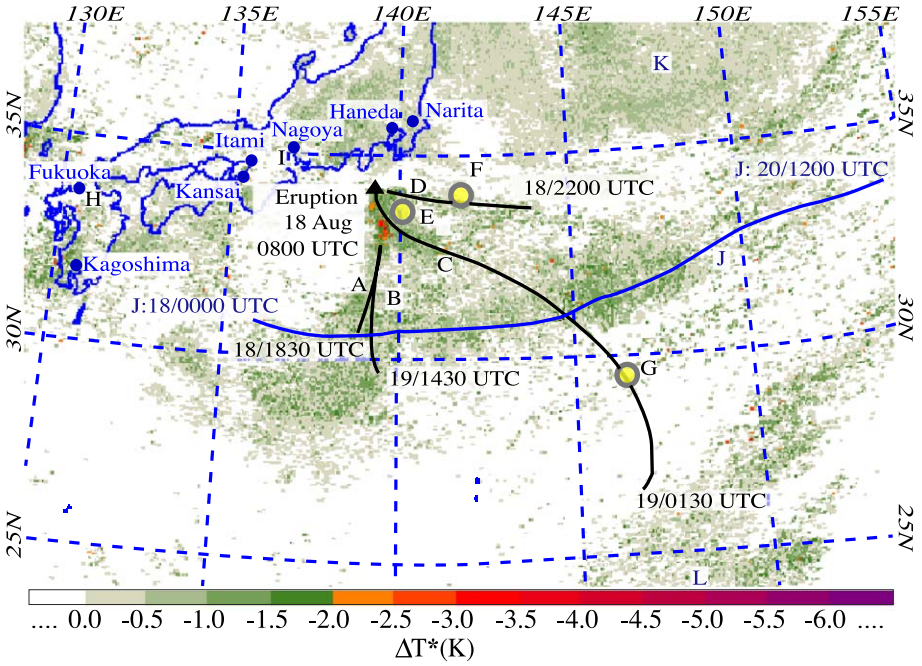

Fig. 5. Miyakejima eruption. Temporal composite of GMS-5/VISSR ΔT*s from 0840 UTC, 18 August 2000, to 2340 UTC, 19 August 2000. Features A–L are described in the text. Major Japanese airports are marked; the busiest are Haneda (domestic) and Narita (international), which service the Tokyo region.

Table 2
Aircraft encounters referred to in text

Event	Date/time	Location	Aircraft	Observations	Damage	Ref. Fig.	Assessed Severity
Miyakejima (1)	18 Aug 2000, 0850 UTC	Not reported (assumed SE of eruption through circumstantial evidence)	DC-10	No report	No report	'E', Fig. 5	N/A
Miyakejima (2)	18 Aug 2000, 0900 UTC	Not reported, but directly following DC-10 above, on descent into Narita.	737–800	Electronic engine controls failed but engines still functioned. Cockpit filled with haze and dust. Flight management computer failed. Emergency landing.	Engine damage, lost forward visibility on windscreen except for a small area under windshield wiper. Leading edges and tail abraded, radome, air data probes damaged. Both engines replaced. Cost US $5 million (Rossier, 2002).	'E', Fig. 5	3
Miyakejima (3)	18 Aug 2000, 0930 UTC	34:00 N 140:30 E	747	Encountered ash cloud at 34,000 ft (10.3 km), exited cloud at 30,000 ft (9.1 km) 2 minutes later. Emergency landing.	3 engines, flight deck wind screen, some forward passenger windows replaced. Fourth engine to be replaced after 100 hours flying time. Cost>US $5 million.	'E', Fig. 5	3
Miyakejima (4)	18 Aug 2000 1235 UTC	33:54 N 142:09 E	747	Aircraft had diverted east of normal track to attempt to evade ash cloud. Strong sulfuric smells, 'sparking' on windshield.	Aircraft removed from service and inspected for three days, but no ash found. Cost to airline of diversions/ inspections>US $2 million.	'F', Fig. 5	0–1
Miyakejima (5)	18 Aug 2000 2010 UTC	28 N to 30 N, 430 nm east of volcano	747	Sulfuric smells	Nil	'G', Fig. 5	0
Manam, Langila, Rabaul	12 Feb 1997, 1129 UTC	8:45 S 144:30 E	747	Smell of sulfur, apparent temperature rise, radio interference	Nil	Fig. 9d	0

Encounter severities assessed from USGS scale (ICAO, 2001). Note: some aviation sources have suggested that the costs associated with the Miyakejima encounters may have been considerably more than the figures quoted here.

expected to be, suggesting high level SO_2 was associated with the ash.

Cloud B moved on a similar path but much more slowly. Comparison with upper winds suggests that this cloud was at levels of about 5–8 km, moving southwards at 4 m/s. Fig. 6 is a comparison of the VISSR and MODIS split window products at 0040 and 0105 UTC on 19 August, showing the developing low and cloud B (green) as it moved south and was entrained into the low. The MODIS image is less noisy and shows slightly

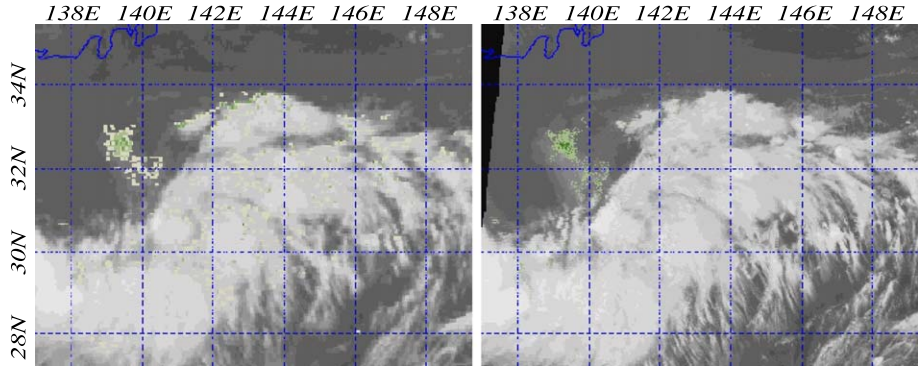

Fig. 6. Miyakejima eruption. Comparison of GMS-VISSR ΔT^*/IR1 (left) and Terra/MODIS ΔT^*/T31 (right) images at 0040 UTC and 0105 UTC respectively on August 19, 2000. Scaling for negative ΔT^*s as for Fig. 5. Cloud B from Fig. 5 is evident (green) on both images, moving SSE from Miyakejima and being drawn into a developing low pressure system.

stronger ΔT*s than VISSR. Visible images from the same time show lower level eruptions from Miyakejima continuing, and moving westwards over Japan.

Cloud C (Fig. 5) moved southeast at about 25 m/s at levels of 9–11 km, corresponding to the cruising levels at which aircraft encounters at E and G (Fig. 5 and Table 2) are known to have occurred. Detection of this cloud was initially hampered by some diffuse cirrus cloud from storms over Japan earlier in the afternoon, by the moist air into which the eruption occurred (similar to the case described by Simpson et al. (2002)), and presumably also by water present in the phreatomagmatic eruption column (Rose et al., 1995). However, weak ΔT*s of -1.5 to -2.0 K were visible in the plume until it moved over the developing low at 1230 UTC, which although 35 K warmer than the eruption cloud at that stage, presented a sufficiently cold background to inhibit detection (Prata et al., 2001) when combined with the other factors. Subsequent imagery interpretation is highly subjective, and further complicated by scattered maritime cumulonimbus, associated with the developing low, penetrating the eruption cloud and presumably lofting some ash to higher levels.

Cloud D appeared to be quite diffuse, with an altitude of about 8–9 km. Although the encounter at F occurred relatively close to the eruption and the observed phenomena indicated ash in the cloud, no damage was reported following the aircraft inspection.

An EP TOMS AI image from 0044 UTC on 19 August (not shown) had weak features corresponding with clouds C and D. The 0221 UTC overpass to the west of that area gives a strong ash signal clearly associated with cloud B, which probably contained the bulk of the aerosols from the eruption. The overall pattern of dispersion suggested by the TOMS AI images is similar to that predicted by HYSPLIT and VAFTAD output. Both dispersion models suggested a very wide area of ash dispersal to the southeast of, and over, Japan. However, poor temporal resolution and an apparent area of aerosols to the south–southeast of Kyushu limit interpretation of the TOMS AI images.

Many false alarms on the VISSR images appeared in or at the edges of cloud associated with the rapid intensification and passage of a sub-tropical low pressure system (J in Fig. 5), a decaying typhoon to the north (K), and cloud associated with an upper tropospheric disturbance (L). These false alarms were an issue when tracking clouds C&D because of the relatively low signal-to-noise ratio deriving from the factors described earlier.

Finally, lidars recorded aerosols on 23 August at Fukuoka and Nagoya (H and I respectively), at altitudes of 17.5 and 16 km, respectively (Smithsonian Institution, 2000). Dispersion model outputs are quite consistent with high-level ash being advected over Japan some time after the eruption. Convective transport in the atmosphere (described earlier) could be responsible for lifting ash to 17.5 km, if the actual eruption did not attain that height.

3.3.1. Factors contributing to the Miyakejima aircraft encounters

Table 3 presents a chronology of significant events during the initial phases of the eruption. We provide here a brief assessment of IAVW performance:

(1) Encounters 1–4 occurred in areas where the volcanic clouds were well defined by pattern analysis (1–3) or reverse absorption (4), although the first two encounters occurred before the ingestion of the first image was completed. At this stage of the eruption, the eruption cloud and height was viewed by ground based observers, radar and pilots.
(2) Warnings were issued relatively quickly, but at some stage, the communication processes broke down. Air traffic controllers appeared to be using a superseded advisory from Tokyo VAAC and diverted aircraft into the high-level ash cloud C. SIGMETs, the official warnings for international aviation, were not universally received, contained no forecast ash cloud tracks and insufficient height information, and were sometimes slower to be issued than the domestic ARMADs (Table 3). The process between identifying an eruption and issuing an appropriate SIGMET can be complex; Hufford et al. (2000) discuss issues relating to SIGMETs and volcanic ash clouds.
(3) The encounters all happened to foreign airlines, which found it difficult to get reliable information. Domestic carriers had no encounters (N. Todo, JAL, personal communication) and their greater awareness of the state of the volcano enabled them to take appropriate evasive action.
(4) Dispersion models forecast the ash over the location of encounter 5, but warnings had ceased for this area because the ash was no longer detectable; this is both a procedural and a remote sensing difficulty.

3.4. Ruang, 24–26 September, 2002

Fig. 7 shows approximate paths of the principal eruption clouds from the Ruang eruption. Analysis of this case is aided by very good satellite coverage (the eruption occurred shortly after Aqua MODIS became operational), and unusually good meteorological data for the area. For example, during the early stages of the eruption, a radiosonde from Manado (WMO station 97014, just south of Ruang), reached a pressure of 20 hPa (approximately 24 km). Heights of clouds given come from a variety of techniques (Table 1), but principally by correlating cloud drifts with radiosonde winds.

Images from this eruption are also shown in Davey et al. (2003), Tupper et al. (2003), and Tupper and Kinoshita (2003). The eruption began with a bifurcated plume between 3 and 5 km high, seen on visible imagery from 2240 UTC on 24 September, and drifting westwards at 5–8 m/s with weak ΔT*s and reaching location ‘A’ (Fig. 7) before

Table 3
Selected chronology of the initial stages of the Miyakejima eruption (after Smithsonian Institution, 2000, 2002a; Tokyo VAAC and Narita JMA logs; Rossier, 2002; confidential airline reports and personal communications)

8 July 2000	Initial crater collapse-explosions and other activity continue through to 18 August.
18 Aug 0802 UTC	Eruption at Miyakejima, top to 2.8 km. Tokyo VAAC received notification at 0805 UTC.
18 Aug 0812 UTC	Tokyo VAAC received observation from JMA Miyakejima observatory; eruption now >5.8 km.
18 Aug 0815 UTC	Tokyo VAAC issues Volcanic Ash Advisory 1: eruption >19,000 ft (5.8 km). Either now or at 0830 ???? UTC, volcanic ash chart for domestic area issued, forecasting ash movement to south, below 30,000 ft (9 km). This chart was subsequently used by Air Traffic Control for avoidance procedures during the event.
18 Aug UTC	NOTAM (notice to airman) RJTD A3781/00 advises ash cloud tops to 5.8 km.
18 Aug 0820 UTC	JMA Haneda issues ARMAD 1 (area meteorological advisory) for domestic aircraft: Volcanic ash observed at 0802 UTC, tops to 5.8 km, movement unknown, intensity unknown.
18 Aug 0825 UTC	JMA Narita issues SIGMET 1: Volcanic ash observed at 0802 UTC, tops to 5.8 km, movement unknown, intensifying.
18 Aug 0825 UTC	Pilot report received at Tokyo VAAC; eruption >25,000 ft (7.6 km) at 0810 UTC.
18 Aug 0830 UTC	Pilot report received at Tokyo VAAC; eruption 40,000 ft (12 km) at 0829 UTC.
18 Aug 0833 UTC	Meteorology office of airline with encounter (3) issues report of eruption to 5.8 km.
18 Aug 0835 UTC	Tokyo VAAC issues Volcanic Ash Advisory 2; eruption 40,000 ft (12 km) extending SE. No further details are given due to time constraints.
18 Aug 0840 UTC	SIGMET 2: Volcanic ash over Miyakejima observed by Boeing 747 at 0829 UTC, tops >12 km, drifting ESE, intensifying. One airline reported that this was the only SIGMET received. ARMAD 2 issued at the same time with same information.
18 Aug 0846 UTC	Revised NOTAM RJTD A3782/00 advising ash to 40,000 ft (12 km).
18 Aug 0850 UTC	Encounter (1) near E, Fig. 5.
18 Aug 0855 UTC	SIGMET 3: Volcanic ash from Miyakejima observed by Boeing 747 at 0829 UTC, tops >12 km, drifting ESE, intensifying.
18 Aug 0900 UTC	Encounter (2) near E, Fig. 5.
18 Aug 0915 UTC	Tokyo VAAC conducts analysis of first GMS/VISSR image, overpass time approx 0840 UTC (image probably available ~ 0905 UTC), runs dispersion model, formulates policy.
18 Aug 0925 UTC	Tokyo VAAC issues Volcanic Ash Advisory 3 (height of eruption 46,000 ft (14 km), with 18 h dispersion forecast. Volcanic ash nephanalysis, forecast charts issued for domestic users only.
18 Aug 0930 UTC	Encounter (3) near E. Aircraft had requested diversion, which was only partially allowed.
18 Aug 1155 UTC	Tokyo VAAC issues Volcanic Ash Advisory 4 (height of eruption 47,000 ft (14.3 km), with 18 h dispersion forecast. Volcanic ash nephanalysis, forecast charts issued for domestic users only.
18 Aug 1206 UTC	Aircraft associated with encounter (4) departs Narita.
18 Aug 1235 UTC	Encounter (4) near F, Fig. 5.
18 Aug 1420 UTC	Volcanic Ash Advisory 5: Ash height 12.5 km, full dispersion forecast given.
18 Aug 1430 UTC	ARMAD 3: Volcanic ash from Miyakejima, tops 12.5 km, drifting ESE, no change in intensity.
18 Aug 1440 UTC	SIGMET 4: Volcanic ash from Miyakejima, tops 12.5 km, drifting ESE, no change in intensity.
18 Aug 1535 UTC	Encounters 2 and 3 reported on NHK television news.
18 Aug 1800 UTC	Volcanic Ash Advisory 6: Ash height 10.7 km, full dispersion forecast given.
18 Aug 1920 UTC	Tokyo VAAC analysts note difficulty of tracking dispersing ash cloud because of cumulonimbus overlap.
18 Aug 2010 UTC	Encounter (5) near G, Fig. 5.
18 Aug 2015 UTC	Volcanic Ash Advisory 7. High level eruption cloud is no longer trackable and advisory focuses on lower level ash, max height 5.8 km (cloud B in Fig. 5).
18 Aug 2030 UTC	ARMAD 4 and SIGMET 5: Volcanic ash from Miyakejima, tops 5.8 km, movement unknown, intensity weakening.
After 18 Aug	Airline reports 'Flow NOTAMs' specifying safe route of passage take aircraft directly over volcano while still in eruption.

being obscured by the main eruption cloud at 0545 UTC on the 25th.

The main eruption had actually begun at 0340 UTC on the 25th (Dali Ahmad, Indonesian Directorate of Volcanology and Geological Hazard Mitigation, personal communication). This eruption cloud was observed to split into four chief parts at altitudes above freezing level (4 km); Cloud B, in a deep layer between 5 and 14 km in height (encompassing aircraft cruising levels), drifted steadily west at 16 m/s in the middle to upper troposphere and gave a discernable ΔT^* signal through to 2345 UTC on 26 September, when it was over Malaysia's Sarawak province, 1300 km west of Ruang and 44 h after the main eruption. Cloud C was at about 14–16 km, just below the tropopause, in a layer moving southwest at 16 m/s. This cloud clearly contained ash (Tupper et al., 2003) and probably also contained a significant amount of ice, with a diffusing cirrus-like cloud faintly visible until about 2240 UTC on 25 September over southern Sulawesi (but little ΔT^* signal).

Cloud D was probably mainly stratospheric, between 16 and 18 km, and drifted westwards at only about 2–3 m/s, remaining visible on VISSR ΔT^*/IR1 imagery until approximately 1945 UTC on 26 September, 40 h after the main eruption. The split window signal for this cloud was strong ($\Delta T^* < -5.5$ K). We postulate that the core of the eruption cloud contained relatively little water, and that substantial amounts of ash penetrated into the dry stratosphere. Further work to explore the microphysical evolution of the cloud is planned.

Interestingly, MODIS ΔT^*s for D (but not B) were consistently of a smaller magnitude than the equivalent GMS images (Fig. 8) or AVHRR images (Tupper et al., 2003). Multispectral images using the MODIS 8.4–8.7 μm and 7.2–7.5 μm bands indicate a strong SO_2 content in

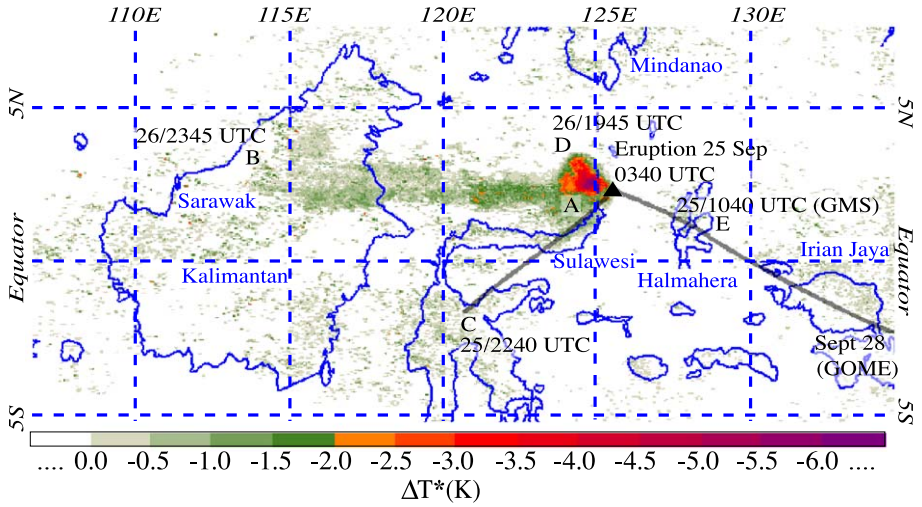

Fig. 7. Ruang eruption. Temporal composite of GMS-VISSR ΔT^* images from 22:40 UTC 24 September 2002 to 1945 UTC 26 September 2002, showing clouds dispersing from eruption at Ruang. Features A to E are described in text.

cloud D but not in the lower clouds (Davey et al., 2003); the different instrument responses for 11/12 μm for cloud D suggest that the relatively narrow MODIS 10.8–11.3 and 11.8–12.3 μm channels are less sensitive to non-ash components than their broader VISSR and AVHRR equivalents. Again, this possibility will be the subject of further investigation.

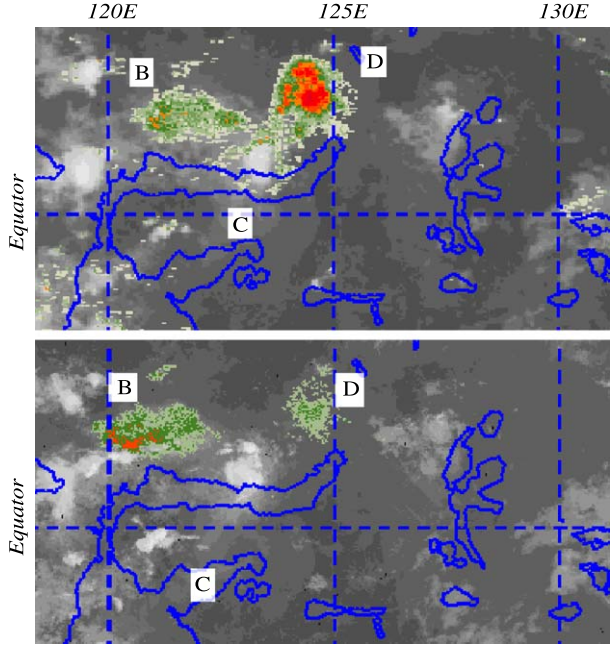

Fig. 8. Ruang eruption, 25 September 2002. Comparison of 1245 UTC GMS-VISSR ΔT^*/IR1 (above) with 1415 Terra/MODIS ΔT^*/31 (below). The differences of detection for cloud 'D' are slightly exaggerated here because of the image time difference (there was a GMS data gap at 1345 and 1445), but are still representative of comparisons throughout the eruption. Scaling for negative ΔT^*s is as for Fig. 7.

Finally, cloud E moved eastwards in the stratosphere at about 16 m/s, at between 18 and approximately 22 km in height. The cloud gave no ash signal using any technique and is seen only as a faintly distinguishable cloud on IR imagery until 1040 UTC on 25 September, before it was advected above thunderstorm cloud tops over Halmahera. SO_2 anomalies apparently associated with clouds D and E were detected with Global Ozone Monitoring Experiment (GOME) imagery in the New Guinea area from 26 until 28 September (University of Bremen, http://www-iup.physik.uni-bremen.de/gomenrt/). We assume Cloud E was mainly gaseous with only trace amounts of ash.

EP TOMS data for the eruption was limited by inter-orbit data gaps, inevitable from a single polar orbiting satellite over an equatorial eruption. Cloud B was well detected on EP TOMS AI imagery over eastern Kalimantan at 0347 UTC on 26 September, with another area of aerosols over south-western Kalimantan thought to be associated with biomass burning. Clouds D and E were initially not observed due to data gaps, and no SO_2 was observed moving eastward over the next few days. We believe that this reflects GOME's higher sensitivity to small SO_2 amounts despite a relatively large footprint.

Operationally, in addition to the relatively strong remote sensing performance, Ruang was the first major Indonesian eruption where eruption information was relayed to the VAAC before the eruption climax. A negative aspect was that no SIGMETs were received from the relevant Meteorological Watch Office, so some airlines continued to fly through the affected areas. The stratospheric cloud E was not identified in real-time and airlines flew underneath it; even though it was far higher than cruising levels and probably contained little ash, many airlines prefer to avoid this situation because of the possible fallout from the cloud

(G. Rennie, Qantas, personal communication). Air traffic controllers relied on Volcanic Ash Advisories for airspace management and the diffusing tropospheric ash clouds caused considerable disruption as they approached Jakarta and Singapore. Although no aircraft encounters with volcanic ash were reported, this disruption alone would have caused millions of dollars in extra costs for the aviation industry.

3.5. Manam, Langila and Rabaul, 8–14 February 1997

Manam, Langila and Rabaul were active for most of February 1997, with regular post-event reports received for the three volcanoes from Rabaul Volcano Observatory (RVO), and real-time pilot reports received for the Langila eruptions. Observations of all kinds were affected by the extent of convective activity.

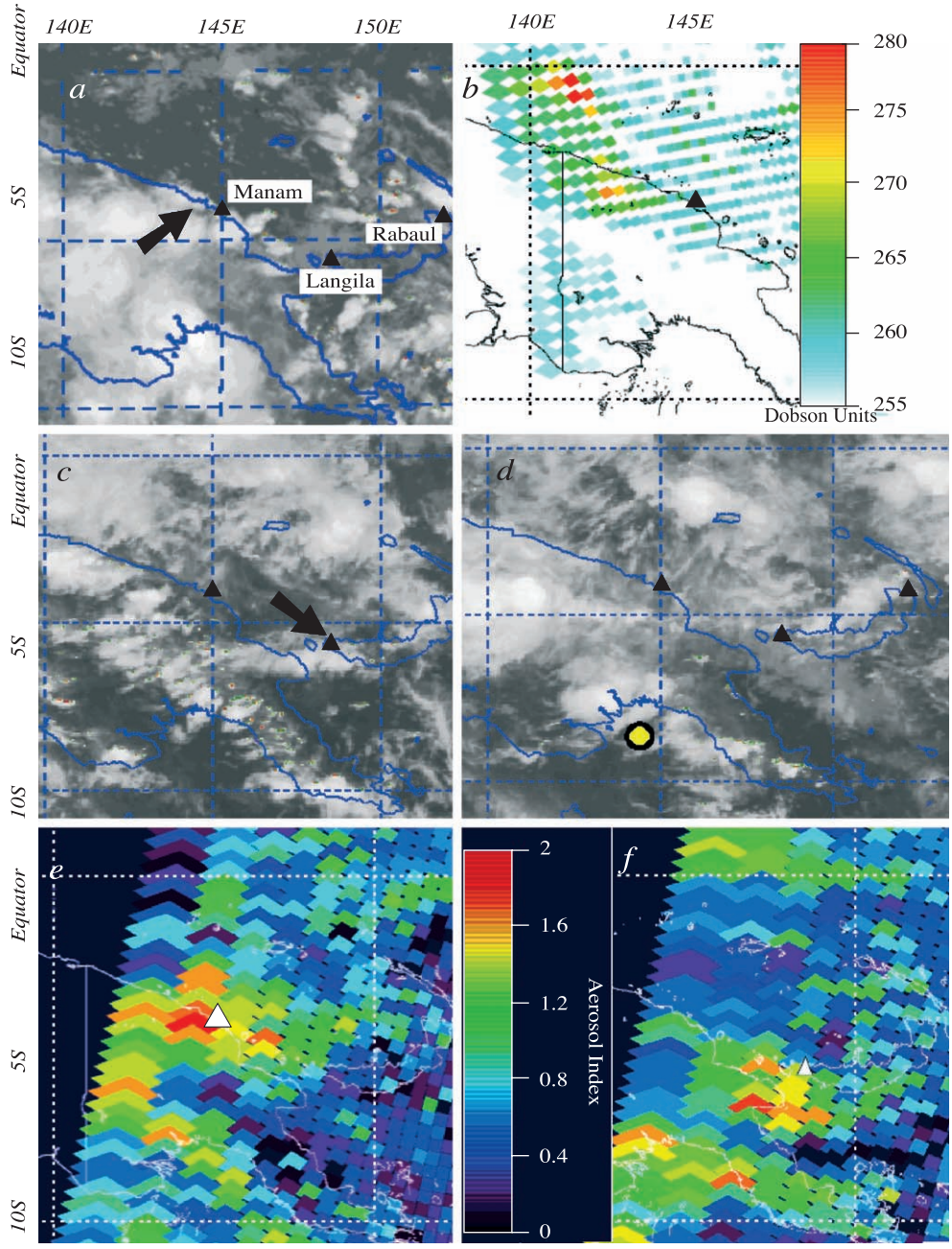

Fig. 9. Selected eruptions detected during February 1997. (a) GMS-5/VISSR ΔT*/IR1, 8 Feb 1997, 1445 UTC, showing eruption plume (arrowed) from Manam, scaling for negative ΔT*s as for Fig. 7. (b) EP TOMS O_3 image, 9 Feb 1997, 0136 UTC, showing dispersal of gas to west of Manam. (c) GMS-5/VISSR ΔT*/IR1, 12 Feb 1997, 0645 UTC, (d) GMS-5/VISSR ΔT*/IR1, 12 Feb 1997, 1145 UTC (e) ADEOS TOMS AI, 10 Feb 1997, 0020 UTC, with aerosols west of Manam (marked), and between Manam and Langila. (f) ADEOS TOMS AI, 14 Feb 1997, 0014 UTC, with ash probably principally from Langila (marked).

Volcanic ash could not be definitely identified using reverse absorption imagery during February 1997 using GMS or AVHRR data, despite frequent explosive eruptions from these volcanoes. The ΔT*/IR1 VISSR composite (not shown) displayed a number of false alarms resulting from channel misalignment (Prata et al., 2001), but little else of interest. Pattern analysis of IR and visible imagery identified two or possibly three eruptions in post-analysis with comparison to ground and pilot reports, but not in real-time. TOMS SO_2, Ozone, and AI images were more effective, although limited by the low data frequency.

Fig. 9a shows an eruption plume from Manam, first identified in non real-time ground reports and then found in GMS IR imagery and TOMS data (Fig. 9b) during post analysis. On GMS IR animations, the eruption was first visible at 1145 UTC on 8 February, and was traceable only for a few hours. ADEOS and EP TOMS ozone data indicated SO_2 from the eruption dispersing westwards the next day at 0047 UTC and 0136 UTC respectively. Ground reports described strong eruptive activity to 7 km, between 0610 UTC and 1730 UTC on 8 February, with dark ash laden clouds blown south by low level winds. IR temperatures suggest a height of about 16 km (i.e., close to the tropopause) during the night. This height would have been virtually impossible to estimate accurately from the ground, and especially at night (Tupper & Kinoshita, 2003). Rabaul also erupted on 8 February, reported to 7 km height by ground observers (Smithsonian Institution, 1997). Deep convection formed over Rabaul during the afternoon and persisted for longer than usual, but this cannot be definitely attributed to the eruptions. No records are available of the timing of explosions from Rabaul on that day (Ima Itikarai, RVO, personal communication, 2003).

ADEOS TOMS AI imagery showed an aerosol maximum just west of Manam on 10 February at 0020 UTC (Fig. 9e) and an ADEOS TOMS O_3 image indicated areas of SO_2 on the 11th at 0134 UTC, with maxima east and west of Manam and over southern Papua New Guinea. Ground reports for this period were of continuous gray to dark ash-laden clouds to 7 km height from Manam, ash clouds to 5 km from Langila, and to 2 km from Rabaul. No ash clouds were identifiable on GMS or NOAA imagery during this period.

Fig. 9c and d show an eruption from Langila, on 12 February, and the location of a subsequent aircraft encounter (Table 2). Tupper and Kinoshita (2003) show a GMS-5 visible image from this eruption, which appears identical to nearby thunderstorm cloud. During the 12th, pilots reported a ‘solid core of discernable ash to 8 km, ash plume of tight radius’ (0630 UTC) from Langila, and ash ‘more than 8 km in height’ (0816 UTC). Ground observers reported eruption heights to 10 km from Langila, 4 km from Manam, and 2 km from Rabaul. Backward trajectories and post-analyzed charts suggest Langila as the most likely source for the ash from the encounter, but are not conclusive as the expected trajectory from Langila was north of the position of the encounter. No ash or SO_2 was detected in the vicinity of the encounter by any method.

Finally, ADEOS TOMS detected aerosols southwest of Langila, and far to the northwest, at 0014 UTC on 14 February (Fig. 9f). Reports from RVO around this time indicate ash to 5 km at Langila on the 13th, and to 4 km at Rabaul and 3 km at Manam on the 14th.

We scrutinized scatter diagrams for all available NOAA and GMS data during this period (Prata et al., 2001), and found no evidence for positive ΔTs from water vapor obscuring negative ΔTs from un-glaciated ash cloud. Some scatter diagrams for the Langila plumes may show mixed ash and water/ice characteristics, but the data are ambiguous. If we exclude the unlikely circumstance that eruptions from all three volcanoes contained unusually high amounts of water (Rose et al., 1995), then the poor detection can be presumed due to a combination of obscuration by overlying cloud, and glaciation from water/ice entrained from the moist atmosphere.

4. Discussion

4.1. Eruption detection issues

The high temporal resolution of geostationary satellites has been very important in the development of the IAVW. Had no ground based observations been available, all eruptions described herein, apart from those of Manam, Langila and Rabaul, could have been detected on the first available image using either pattern recognition or reverse absorption. The exceptions from Papua New Guinea are important; a reliable eruption detection system cannot be dependent on the meteorological conditions and it is necessary to have a weather-independent warning capacity. At the time of writing, ground-based monitoring of Langila has ceased (Wally Johnson, Geoscience Australia, personal communication), and monitoring activity at Manam has been rendered extremely difficult because of resource and socio-political issues (Tupper & Kinoshita, 2003).

A strong benefit of ground-based seismic observations is that they can be used for eruption prediction, and it is thus possible to implement conservative aircraft routing strategies and develop contingency plans to ensure a robust crisis response. The confusion at Miyakejima illustrates this perfectly; foreign airlines had little pre-eruption information and suffered from an imperfect, reactive warning system despite the fast initial reaction time, while local airlines, who had detailed contingency plans and better information flow, were able to operate safely. That this extremely dangerous situation occurred in one of the world’s most technologically advanced and volcanically aware countries, should serve as an illustration of the progress yet to be made in the IAVW and a forewarning of the likely performance of the system in other parts of the world.

We believe that ground-based detection, through seismic, infrasonic and other monitoring, is essential for the development of a robust IAVW. While this is a daunting task for remote volcanoes, it is not impossible; for example it is expected that by 2004, 31 of the 43 historically active and remote Aleutian volcanoes will have seismic monitoring (Marianne Guffanti, U.S. Geological Survey, personal communication). Moreover, our experiences are that ground-based observations, clearly and quickly communicated, greatly improve the value to the IAVW of remote sensing observations by giving certainty to the fact of the eruption. However, if these data are not robustly integrated into IAVW procedures, further Miyakejima-type situations are inevitable.

4.2. Performance of remote sensing techniques for volcanic cloud monitoring

4.2.1. Pattern analysis

Single IR and visible channel pattern analysis cannot be used alone to support the IAVW. For those situations where reverse-absorption monitoring is ineffective but the eruption is still seen on imagery, the length of time for which ash cloud can be inferred from pattern analysis is shorter than the IAVW requires. Once dense and cold cloud tops become transparent, and albedo features are weakened as the heavier particles drop out of the ash cloud, it can be very difficult to track volcanic ash cloud with any confidence. Detection periods usually range from about 2–12 h after the eruption. The results here are consistent with the extensive work of Sawada (1987).

4.2.2. The reverse absorption technique

4.2.2.1. GMS-5/VISSR data were highly useful for volcanic monitoring. These cases verify the assertion of Potts and Tokuno (1999) that the high frequency of the GMS-5/VISSR data would be valuable for volcanic cloud monitoring in the region, even though the AVHRR and MODIS data has better spatial and temperature resolution. For each event, there were variations in image quality, especially from the polar orbiting satellites where the ΔT*s and image clarity depended on how favorable each orbit was for observing the eruption. Overall, the VISSR ΔT*s were close to the AVHRR and MODIS data. For eruptions of this size, the high frequency of receipt of GMS/VISSR data far outweighs the poorer spatial resolution of the satellite and the 'noise' resulting from relatively low data precision.

4.2.2.2. False alarm and probability of detection issues. False alarms in these cases were generally associated with poor data precision and/or calibration (for VISSR), and with cloud or clear air under inversions in the troposphere. For the Bezymianny, Shiveluch and Ruang cases, the good signal-to-noise ratio permitted extensive tracking of the majority of ash clouds. For some of the Miyakejima clouds and one of the Ruang clouds, the signal was sufficiently reduced by the inhibiting factors described in the text for ash/noise discrimination to be an issue. The eruptions from Papua New Guinea presumably had ice-dominant cloud tops and no detectable ash signal using reverse absorption. The inhibiting factor of positive ΔT*s from high water vapor loading appeared to have the beneficial side effect of reducing the level of false alarms, especially for the Ruang case. This was difficult to evaluate for the Miyakejima case, where the atmosphere was also moist, because the VISSR data were particularly noisy.

4.3. Eruptions and moist convection

Eruption clouds exist on a spectrum between the 'volcanic thunderstorm' (Oswalt et al., 1996) and a volcanic cloud relatively unaffected by environmental interactions. In the moist tropics, we would expect that entrainment of water vapor and the higher tropopause will increase the height of maximum ascent of otherwise small to moderate sized eruptions, resulting in high eruption clouds with high water vapor but relatively less ash (Graf et al., 1999; Woods, 1993), and therefore a proportionally lower chance of detection than an eruption of the same height at high latitudes. Rabaul Volcano Observatory has observed convective growth over small eruptions in Papua New Guinea (Ima Itikarai, personal communication, 2002), and Tupper and Kinoshita (2003) show large cumulus forming over passive degassing in a moist environment at Sakurajima, Japan.

From the satellite perspective, eruptions of Manam on 5 October 1998, and of Ulawun on 30 April 2001, were very similar to the Papua New Guinea cases presented here, with a cloud ascending close to the tropopause, SO_2 clearly detected by TOMS, but no ash found with the split-window algorithm. These eruptions may be regarded as circumstantial evidence of enhanced volcanic cloud height through radial entrainment, but much more work needs to be done on the subject.

Another result of the convective process is that 'masking' cloud can form at the top of the ash cloud, either as a pileus cloud during rapid ascent or as a cirrus anvil over a mature, deep cloud, and obscure the ash present in the cloud below. Hoblitt et al. (1996) show photographs of pre-paroxysmal eruptions of Pinatubo where this effect is noticeable. Cumulonimbus anvils are usually persistent for several hours after thunderstorm formation, well after the rest of the cloud has dissipated, and form an effective barrier to satellite monitoring.

Enough eruptions have been recorded in Papua New Guinea in recent years to show that application of current operational techniques is very difficult. If it were not for the exceptional work of the Rabaul Volcano Observatory and the equally important pilot reports from Air Niugini and other airlines, then many, if not most, eruptions would have been completely undetected.

4.4. Future improvements in IR detection

Although the limiting effects described earlier will remain, IR detection is still likely to improve. Tokuno (2000) shows how split-window detection with MTSAT can be expected to give stronger ΔTs than GMS-VISSR and NOAA-AVHRR satellites. The data precision will also be higher, which will result in less background noise, and the capacity to perform 'fine-tuning' such as water vapor corrections. The net effect of these improvements will be to reliably sense more of each ash cloud, and to sense the ash clouds to a greater distance and time from their source. In addition, the availability of a 3.7-μm channel on MTSAT will enable implementation of 3-channel techniques (Ellrod et al., 2003) to better detect volcanic clouds, as well as further research into improved uses of short-wave IR channels for future satellite sensors.

New multi-channel radiometers (e.g. MODIS, GLI, SEVIRI) offer interesting possibilities for improved volcanic ash detection. A channel near 8.6 μm can be used to detect ash when used in combination with a second longer wavelength channel, and can also be used to identify low level SO_2 (Realmuto et al., 1994). Prata, Rose et al. (2003), Prata, Watson et al. (2003) and Rose et al. (2003) have recently shown that the 7.3 μm channel can be used to quantitatively measure the SO_2 column abundance in the upper troposphere/lower stratosphere. Such data have been routinely available since 1979 from the HIRS family of instruments, on board the NOAA satellites. These new channels for ash/SO_2 detection are available on MODIS and SEVIRI. The AIRS instrument on board the Aqua platform offers another exciting possibility for ash/SO_2 detection. This instrument provides more than 2000 channels, with key ash/SO_2 channels situated around 4, 7.3, 8.4 μm and in the 10–13 μm window. Carn et al. (2002) have compared IR SO_2 retrievals with TOMS. The great utility of these new IR techniques is that they complement the well-established UV methods (e.g. TOMS and GOME) and they fill the nighttime SO_2 measurement gap.

4.5. TOMS and GOME data

Despite the low data frequency, TOMS AI, SO_2 and O_3 products have significantly added to the analysis of these events. In particular, the ability of TOMS to detect aerosols and SO_2 near and above the top of moist tropical cloud masses has great potential for operational use. Meteor-3 TOMS AI and SO_2 images also enabled tracking of the 1994 Rabaul eruption cloud for several days, despite the seawater interaction that prevented observation with the reverse absorption technique (Rose et al., 1995).

The most obvious way to expand the use of this type of data is to mount a UV TOMS-like instrument on a geostationary platform. Unfortunately, recent proposals to trial this configuration have been unsuccessful, perhaps due to the night-time data gap. However, based on the events studied here, and particularly the eruptions in Papua New Guinea, which lies in the region of the warmest sea surface temperatures, most moist air and greatest high cloud cover in the world, the daytime data collected would more than justify the launch of such an instrument. Similar conditions are prevalent in Indonesia, the Solomon Islands and the Philippines for most of the year.

Part of the value of TOMS is its capacity to simultaneously sense ash and SO_2, although both are subject to false alarms from other sources. SO_2 data are not yet widely used in the IAVW, because of the delay in obtaining the data, and because the focus of the system is on volcanic ash. However, if the data were available frequently and in real-time, it could be used directly in volcanic ash warnings by making one reasonable assumption: the presence of SO_2 near a known eruption should imply at least trace levels of ash at the level of the SO_2, and, for a high level SO_2 cloud, significant quantities of ash dispersing at lower levels.

This assumption is certainly valid for the latter three events examined here, and is consistent with other studies (e.g. Constantine et al., 2000). Ellrod et al. (2002) point out that SO_2 is a recognized source of aviation damage in its own right. Hence SO_2 detection should form part of operational IAVW procedures, and may, when combined with dispersion model analysis, provide a partial solution to the obscuration of lower level ash by cloud.

4.6. A holistic approach to volcanic cloud detection

It is quite clear from the cases considered here that there remains a high potential for an aviation tragedy as a result of a volcanic eruption. This might result from human error, data sparseness, communication problems, dispersion model problems, or weaknesses in remote sensing. In all likelihood, it would result from a combination of a number of these factors.

Constantine et al. (2000), comparing TOMS and AVHRR data for the eruption of Cerro Hudson in 1991, asserted that each detector has advantages that apply in different environmental conditions, and that each should be used in a (partially) 'redundant but complementary volcanic-cloud mitigation effort'. We affirm this view. We also assert that more work needs to be done overall on the IAVW. We strongly advocate a holistic approach to ash detection and warning, which recognizes the advantages and drawbacks of the various technologies outlined in this paper. These will include automated satellite detection, meteorological analyses, pilot reports, dispersion modeling, seismic and other geophysical pre- and post-eruptive data, and ground-based measurements (e.g. observers' reports, earthquake data, web-cam information). We advocate the use of new methods alongside existing techniques and expect that in the near future on-board detection instruments will be available as well as operational ground-based IR cameras providing real-time volcanic ash/SO_2 imagery.

5. Conclusions

We have examined the ability of all available data to describe the dispersion of volcanic clouds in the western Pacific region during five major events involving eruptions from eight volcanoes to or above the cruising level of aircraft on international routes. We show:

(a) No single method of observation or satellite sensor is able to identify and track volcanic clouds in every case. The principal limitations affecting detection are the presence of meteorological cloud obscuring eruptions, or of substantial amounts of ice in volcanic clouds. In cloudy conditions, one cannot sufficiently monitor volcanic clouds using remote sensing alone. Two of the six aircraft encounters described occurred in conditions where the volcanic cloud could not be clearly identified by remote sensing.
(b) Currently, the best method for discriminating dispersing volcanic ash clouds from water/ice clouds is the reverse absorption, or split-window technique. We were able to track one eruption cloud in this study for 80 hours using this technique on GMS-5/VISSR imagery.
(c) Hourly animation of GMS-5/VISSR reverse absorption images provided better tracking of volcanic clouds than using NOAA/AVHRR and (single channel) GMS-4/VISSR data combined.
(d) TOMS data showed skill in detecting volcanic SO_2 or ash at the top of volcanic clouds not well detected with the reverse-absorption technique. A TOMS-like instrument on a geostationary platform would be a valuable tool for operational volcanic cloud sensing. Better use can be made of SO_2 data for implying the existence of ash.
(e) The enhancement of complementary ground-based observations, and careful collaboration between meteorological and volcanological agencies is necessary because of the certainty of overlying cloud inhibiting remote sensing observations in many future eruptions, and because of the added value of ground-based predictive techniques.

Acknowledgements

This manuscript was greatly improved by the comments of three anonymous reviewers, as well as J. Travers and K. Mackersy (Wellington VAAC) and J. Arthur, G. Garden and M. Kersemakers (Darwin VAAC). Part of this work was done while A.Tupper was a guest of the Physics Department, Faculty of Education, Kagoshima University. The help of K. Kinoshita, N. Iino, M. Koyamada and C. Kanagaki is greatly appreciated. Our colleagues in the relevant VAACs and volcanological observatories assisted with the analysis of these cases, E. Miller, G. Rennie, R. Cantor, and N. Todo provided aviation information, and some airlines anonymously provided details of their volcanic cloud encounters. G.Garden conducted the initial post-analysis of the Langila eruptions. B. Stunder (NOAA Air Resources Laboratory) provided VAFTAD data for some of these cases and others considered for the paper, and P. Stewart of the Bureau of Meteorology's National Meteorological and Oceanographic Centre provided HYSPLIT output. NOAA, the UK Met Office via the British Atmospheric Data Centre, and the University of Wyoming provided radiosonde data. NASA and NOAA provided archived MODIS and AVHRR data, respectively.

References

Ackerman, S. A. (1997). Remote sensing aerosols using satellite infrared observations. *Journal of Geophysical Research*, 17069–17080.

Campbell, E. E. (1994). Recommended flight-crew procedures if volcanic ash is encountered. In T. J. Casadevall (Ed.), *Volcanic ash and aviation safety: Proceedings of the First International Symposium on volcanic ash and aviation safety, Seattle, WA. U.S. Geological Survey Bulletin, vol. 2047* (pp. 151–157).

Cantor, R. (1998). Complete avoidance of volcanic ash is only procedure that guarantees flight safety. *ICAO magazine*, *53*, 18–19, 26.

Carn, S., Prata, A. J., Karlsdottir, S., & Krueger, A. J. (2002). Integrating TOMS and TOVS retrievals of sulfur dioxide in volcanic clouds. *Eos Transactions AGU*, *83*(47) (Fall Meeting Suppl., Abstract VIZA-1417).

Casadevall, T. J. (1994). The 1989–1990 eruption of Redoubt Volcano, Alaska; impacts on aircraft operations. *Journal of Volcanology and Geothermal Research*, *62*, 301–316.

Casadevall, T. J., Delos Reyes, P. J., & Schneider, D. J. (1996). The 1991 Pinatubo Eruptions and Their Effects on Aircraft Operations. In C.G. Newhall, & R. S. Punongbayan (Eds.), *Fire and Mud: eruptions and lahars of Mount Pinatubo, Philippines* (pp. 625–636). Quezon City: Philippines Institute of Volcanology and Seismology, Seattle: University of Washington Press.

Constantine, E. K., Bluth, G. J. S., & Rose, W. I. (2000). TOMS and AVHRR observations of drifting volcanic clouds from the August 1991 eruptions of Cerro Hudson. In P. Mouginis-Mark, J. Crisp, & J. Fink (Eds.), *Remote sensing of active volcanism. Monograph - American Geophysical Union, vol. 116* (pp. 45–64).

Davey, J. P., Tupper, A. C., & Potts, R. J. (2003). Volcanic cloud monitoring issues at the Darwin VAAC. *WMO/ICAO Third International Workshop on Volcanic Ash, Toulouse, France, September 29-October 3, 2003*.

Draxler, R. R., & Hess, G. D. (1998). An overview of the HYSPLIT_4 modelling system for trajectories, dispersion, and deposition. *Australian Meteorological Magazine*, *47*(4), 295–308.

Ellrod, G. P., Connell, B. H., & Hillger, D. W. (2003). Improved detection of airborne volcanic ash using multi-spectral infrared satellite data. *Journal of Geophysical Research*, *108*(D12), 4356.

Ellrod, G. P., Helz, R. L., & Wadge, G. (2002). Volcanic Hazards Assessment. *Report by Committee on Earth Observation Satellites (CEOS) Disaster Management Support Project*, http://www.ceos.noaa.gov/

FAA (U.S.A.) Aviation Weather Directorate. (2001). User Needs Analysis Document: Volcanic Activity. Version 1.0, 5 Sept 2001.

Graf, H., Herzog, M., Oberhuber, J. M., & Textor, C. (1999). Effect of environmental conditions on volcanic plume rise. *Journal of Geophysical Research*, *104*(D20), 24309–24320.

Grindle, T. J., & Burcham, F. W. (2002). Even minor volcanic ash encounters can cause major damage to aircraft. *ICAO Journal*, *57*(2), 1–14, 29.

Grindle, T. J., & Burcham, F. W. (2003). Engine Damage to a NASA DC-8-72 airplane from a high-altitude encounter with a diffuse volcanic ash cloud. *Technical Memorandum NASA/TM-2003-212030*, 22 pp.

Heffter, J. L., & Stunder, B. J. B. (1993). Volcanic ash forecast transport and dispersion (VAFTAD) model. *Weather and Forecasting*, *8*(4), 533–541.

Higurashi, A., & Nakajima, T. (2002). Detection of aerosol types over the East China Sea near Japan from four-channel satellite data. *Geophysical Research Letters*, *29*(17), 1836–1839.

Hoblitt, R. P., Wolfe, E. W., Scott, W. E., Couchman, M. R., Pallister, J. S., & Javier, D. (1996). The Preclimatic Eruptions of Mount Pinatubo, June 1991. In C. G. Newhall, & R. S. Punongbayan (Eds.), *Fire and Mud: eruptions and lahars of Mount Pinatubo, Philippines* (pp. 457–511). Quezon City: Philippines Institute of Volcanology and Seismology, Seattle: University of Washington Press.

Holasek, R. E., Self, S., & Woods, A. W. (1996). Satellite observations and interpretation of the 1991 Mount Pinatubo eruption plumes. *Journal of Geophysical Research*, *101*(B12), 27635–27665.

Hufford, G. L., Salinas, L. J., Simpson, J. J., Barske, E. G., & Pieri, D. C. (2000). Operational implications of airborne volcanic ash. *Bulletin of the American Meteorological Society*, *81*(4), 745–755.

ICAO. (2000). International Civil Aviation Organisation International Handbook on the International Airways Volcano Watch (IAVW)-Operational procedures and contact list. *ICAO Doc 9766-AN/968, First Edition-2000*. Available at: http://www.icao.int/icao/en/download.htm

ICAO. (2001). International Civil Aviation Organisation International Manual on volcanic ash, radioactive material and toxic chemical clouds. *ICAO Doc 9766-AN/954, First Edition-2001*.

ICAO. (2003). Review of relevant outstanding issues from the Second Workshop on Volcanic Ash (Toulouse 1998). *Third International Workshop on Volcanic Ash, Toulouse, France, 29 September to 3 October 2003*.

Iino, N., Kinoshita, K., Iwasaki, R., Masumizu, T., & Yano, T. (2003). NOAA and GMS observations of Asian dust events during 2000–2002. In W. P. Menzel, W. -J. Zhang, J. Le Marshall, & M. Tokuno (Eds.), *Applications with weather satellites. Proceedings of SPIE, vol. 4895* (pp. 18–27).

Iino, N., Kinoshita, K., Koyamada, M., Saitoh, S., Maeno, K., & Kanagaki, C. (2001a). Satellite imagery of ash clouds of the 2000 eruption of Miyake-jima volcano. *Proc. CEReS International Symp. on Remote Sensing of the Atmosphere and Validation of Satellite Data, Chiba, Japan* (pp. 13–18). CEReS Chiba University.

Iino, N., Kinoshita, K., Yano, T., & Torii, S. (2001b). Detection and morphology of volcanic ash clouds from Mt Sakurajima in satellite images. *Proceedings of PSFVIP-3 March 18–21, 2001, Maui, Hawaii, U.S.A* (pp. 1–8) (CD-ROM; F3023).

Japan Meteorological Agency (Tokyo Volcanic Ash Advisory Center) (2003). Collected volcanic cloud case studies using GMS-5 satellite imagery. Published as a technical report on CD-ROM in Japanese, English version (in press).

Johnson, R. W., & Casadevall, T. J. (1994). Aviation safety and volcanic ash clouds in the Indonesia–Australia region. In Casadevall T. J. (Ed.), *Volcanic ash and aviation safety: Proceedings of the First International Symposium on volcanic ash and aviation safety, Seattle, WA. U.S. Geological Survey Bulletin, vol. 2047* (pp. 191–197).

Kinoshita, K., Kanagaki, C., Iino, N., Koyamada, M., Terada, A., & Tupper, A. (2003). Volcanic plumes at Miyakejima observed from satellites and from the ground. In H. -L. Huang, D. Lu, & Y. Sasano (Eds.), *Optical remote sensing of the atmosphere and clouds III. Proceedings of SPIE, vol. 4891* (pp. 227–236). Bellingham, WA, USA: SPIE.

Kinoshita, K., Nishinosono, M., Yano, T., Iino, N., & Uno, I. (1999). Detection and analysis of Kosa using NOAA/AVHRR data (in Japanese). *Conference on Remote Sensing Society Japan*, *26*, 253–256.

Koyama, T., & Hillger, D. W. (2003). Verification of GMS-5 VISSR infrared detectors. In W. P. Menzel, W. -J. Zhang, J. Le Marshall, & M. Tokuno (Eds.), *Applications with weather satellites. Proceedings of SPIE, vol. 4895* (pp. 210–217).

Krotkov, N. A., Torres, O., Seftor, C., Krueger, A. J., Kostinski, A., Rose, W. I., Bluth, G. J. S., Schneider, D. J., & Shaefer, S. J. (1999). Comparison of TOMS and AVHRR volcanic ash retrievals from the August 1992 eruption of Mount Spurr. *Geophysical Research Letters*, *26*, 455–458.

Krueger, A. J., Walter, L. S., Bhartia, P. K., Schnetzler, C. C., Krotkov, N. A., Sprod, I., & Bluth, G. J. S. (1995). Volcanic sulfur dioxide measurements from the Total Ozone Mapping Spectrometer (TOMS) instruments. *Journal of Geophysical Research*, *100*, 14057–14076.

McMillin, L. M. (1975). Estimation of sea surface temperature from two infrared window measurements with different absorption. *Journal of Geophysical Research*, *80*, 5113–5117.

Merchant, C. J., Simpson, J. J., & Harris, A. R. (2003). A cross-calibration of GMS-5 thermal channels against ATSR-2. *Remote Sensing of Environment*, *84*, 268–282.

Murayama, T., et al. (2001). Ground-based network observation of Asian dust events of April 1998 in east Asia. *Journal of Geophysical Research*, *106*, 18,345–18,360.

Oppenheimer, C. (1998). Volcanological applications of meteorological satellites. *International Journal of Remote Sensing*, *19*, 2829–2864.

Oswalt, J. S., Nichols, W., & O'Hara, J. F., 1996. Meteorological Observations of the 1991 Mount Pinatubo Eruption. In C. G. Newhall, & R. S. Punongbayan (Eds.), *Fire and Mud: eruptions and lahars of Mount Pinatubo, Philippines* (pp. 625–636). Quezon City: Philippines Institute of Volcanology and Seismology, Seattle: University of Washington Press.

Pieri, D., Ma, C., Simpson, J. J., Hufford, G., Grindle, T., & Grove, C. (2002). Analyses of in-situ airborne volcanic ash from the February 2000 eruption of Hekla Volcano, Iceland. *Geophysical Research Letters*, *29*, 19-1–19-4.

Platt, C. M. R., & Prata, A. J. (1993). Nocturnal effects in the retrieval of land surface temperatures from satellite measurements. *Remote Sensing of Environment*, *45*, 127–136.

Potts, R. J. (1993). Satellite observations of Mt Pinatubo ash clouds. *Australian Meteorological Magazine*, *42*, 59–68.

Potts, R. J., & Ebert, E. E. (1996). On the detection of volcanic ash in NOAA AVHRR infrared satellite imagery. *8th Australasian Remote Sensing Conference, Canberra, 25–29 March 1996*.

Potts, R. J., & Tokuno, M. (1999). GMS-5 and NOAA AVHRR satellite observations of the New Zealand Mt Ruapehu eruption of 19/20 July 1996. *Preprints 8th Conf on Aviation, Range and Aerospace Meteorology, American Meteorological Soc*.

Potts, R. J., & Whitby, F. (1994). Volcanic ash warnings in the Australian region. In T. J. Casadevall (Ed.), *Volcanic ash and aviation safety: Proceedings of the First International Symposium on volcanic ash and aviation safety, Seattle, WA. U.S. Geological Survey Bulletin, vol. 2047* (pp. 221–228).

Prata, A. J. (1989a). Infrared radiative transfer calculations for volcanic ash clouds. *Geophysical Research Letters*, *16*, 1293–1296.

Prata, A. J. (1989b). Observations of volcanic ash clouds in the10–12 μm window using AVHRR/2 data. *International Journal of Remote Sensing*, *10*, 751–761.

Prata, A. J., Bluth, G. J. S., Rose, W. I., Schneider, D. J., & Tupper, A. C. (2001). Comments on "Failures in detecting volcanic ash from a satellite-based technique". *Remote Sensing of Environment*, *78*, 341–346.

Prata, A. J., & Grant, I. F. (2001). Retrieval of microphysical and morphological properties of volcanic ash plumes from satellite data: Application to Mt Ruapehu, New Zealand. *Quarterly Journal of the Royal Meteorological Society*, *127*, 2153–2180.

Prata, A. J., Rose, W. I., Self, S., & O'Brien, D. M. (2003). Global, long-term sulphur dioxide measurements from TOVS data: A new tool for studying explosive volcanism and climate. In A. Robock, & C. Oppenheimer (Eds.), *Volcanism and Earth's Atmosphere, AGU Geophysical Monograph 139*, 75–92.

Prata, A. J., Watson, I. M., Rose, W. I., O'Brien, D. M., Realmuto, V. J., Bluth, G. J. S., Servranckx, R., & Crisp, J. (2001). Volcanic sulfur dioxide concentrations derived from infrared satellite measurements. *Submitted to Journal of Geophysical Research (Atmospheres)*.

Realmuto, V. J., Abrams, M. J., Buongiorno, M. F., & Pieri, D. C. (1994). The use multispectral thermal infrared image data to estimate sulfur

dioxide flux from volcanoes: A case study from Mount Etna, Sicily, July 29, 1986. *Journal of Geophysical Research*, *99*, 481–488.

Rose, W. I., Bluth, G. J. S., & Ernst, G. G. J. (2000). Integrating retrievals of volcanic cloud characteristics from satellite remote sensors: A summary. *Philosophical Transactions of the Royal Society of London. A*, *358*, 1585–1606.

Rose, W. I., Delene, D. J., Schneider, D. J., Bluth, G. J. S., Krueger, A. J., Sprod, I., McKee, C., Davies, H. L., & Ernst, G. G. J. (1995). Ice in the 1994 Rabaul eruption cloud: Implications for volcano hazard and atmospheric effects. *Nature*, *375*, 477–479.

Rose, W. I., Gu, Y., Watson, I. M., Yu, T., Bluth, G. J. S., Prata, A. J., Krueger, A. J., Krotkov, N., Carn, S., Fromm, M. D., Hunton, D., Viggiano, A. A., Miller, T. M., Ballentin, J. O., Ernst, G. G. J., Reeves, J. M., Wilson, C., Anderson, B. E., & Flittner, B. E. (2003). The February–March 2000 eruption of Hekla, Iceland from a satellite perspective. In A. Robock, & C. Oppenheimer (Eds.), *Volcanism and Earth's Atmosphere, AGU Geophysical Monograph* 139, 107–132.

Rossier, R. N. (2002, February). Volcanic ash: Avoid at all cost. *Business and Commerical Aviation*, 70–71.

Salinas, L. (1999). Volcanic ash clouds pose a real threat to aircraft safety. Preprints, Eight Conference on Aviation, Range, and Aerospace Meteorology, Dallas, Texas. *American Meteorological*, 253–256.

Sawada, Y. (1987). Study on analysis of volcanic eruptions based on eruption cloud image data obtained by the Geostationary Meteorological Satellite (GMS). *Technical Report - Japan Meteorology Research Institute, vol. 22* (335 pp.).

Sawada, Y. (2002). Analysis of Eruption Cloud with Geostationary Meteorological Satellite Imagery (Himawari) (in Japanese with English abstract and figure captions). *Journal of Geography (Japan)*, *111*(3), 374–394.

Simpson, J. J., Hufford, G., Pieri, D., & Berg, J. S. (2000). Failures in detecting volcanic ash from a satellite-based technique. *Remote Sensing of Environment*, *72*, 191–217.

Simpson, J. J., Hufford, G., Pieri, D., & Berg, J. S. (2001). Response to "Comments on 'Failures in detecting volcanic ash from a satellite-based technique'". *Remote Sensing of Environment*, *78*, 347–357.

Simpson, J. J., Hufford, G. L., Pieri, D., Servranckx, R., Berg, J. S., & Bauer, C. (2002). The February 2001 eruption of Mt. Cleveland, Alaska: Case study of an aviation hazard. *Weather and Forecasting*, *17*, 691–704.

Simpson, J. J., Hufford, G. L., Servranckx, R., Berg, J. S., & Pieri, D. (2003). Airborne Asian dust: Case study of long-range transport and implications for the detection of volcanic ash. *Weather and Forecasting*, *18*, 121–141.

Smithsonian Institution. (1997). Reports on eruptions at Manam, Langila, and Rabaul. *Bulletin of the Global Volcanism Network*, *22*, 02.

Smithsonian Institution. (2000). Report on eruptions at Miyakejima. *Bulletin of the Global Volcanism Network*, *25*, 07.

Smithsonian Institution. (2001a). Report on eruptions at Shiveluch. *Bulletin of the Global Volcanism Network*, *26*, 04.

Smithsonian Institution. (2001b). Report on eruptions at Bezymianny. *Bulletin of the Global Volcanism Network*, *26*, 07.

Smithsonian Institution. (2002a). Further report on eruption at Miyakejima, August 18 2000. *Bulletin of the Global Volcanism Network*, *27*, 03.

Smithsonian Institution. (2002b). Report on eruption at Ruang. *Bulletin of the Global Volcanism Network*, *27*, 10.

Sokolik, I. (2002). The spectral radiative signature of wind-blown mineral dust: Implications for remote sensing in the thermal IR region. *Geophysical Research Letters*, *29*, 2154–2156.

Sokolik, I. (2003). Remote sensing of mineral dust aerosols in the UV/visible and IR regions. In H. -L. Huang, D. Lu, & Y. Sasano (Eds.), *Optical remote sensing of the atmosphere and clouds III. Proceedings of SPIE, vol. 4891* (pp. 265–271). Bellingham, WA, USA: SPIE.

Tokuno, M. (2000). MTSAT Window Channels' (IR1 and IR2) Potential for Distinguishing Volcanic Ash Clouds. *Meteorological Satellite Center (Japan) Technical Note No. 38*, 11 pp.

Torres, O., Bhartia, P. K., Herman, J. R., Ahmad, Z., & Gleason, J. (1998). Derivation of aerosol properties from satellite measurements of backscattered ultraviolet radiation: Theoretical basis. *Journal of Geophysical Research*, *103*, 17099–17110.

Tupper, A. C., Davey, J. P., & Potts, R. J. (2003). Monitoring Volcanic Eruptions in Indonesia and the Southwest Pacific (in English with Japanese abstract and figure captions). In K. Kinoshita (Ed.), *Researching Eruption Clouds of Volcanic Island Chains, Kagoshima University, 9–10 November 2002, Kagoshima University Research Center for the Pacific Islands. Occasional Papers, vol. 37* (pp. 153–163).

Tupper, A. C., & Kinoshita, K. (2003). Satellite, air and ground observations of volcanic clouds over islands of the Southwest Pacific. *South Pacific Study*, *23*, 21–46.

Watkin, H. A., Scott, T. R., Macadam, I., Radice, L. C., & Hoad, D. J. (2003). Reducing the false alarm rate of a Met Office automatic volcanic eruption detection system. *UK Met Office Forecasting Research Technical Report, 414*, 19 pp.

Woods, A. W. (1993). Moist convection and the injection of volcanic ash into the atmosphere. *Journal of Geophysical Research*, *98*(B10), 17627–17636.